Fish and Shellfish Immunology 94 (2019) 871–879

Contents lists available at ScienceDirect

Fish and Shellfish Immunology

journal homepage: www.elsevier.com/locate/fsi

Full length article

Grass carp cGASL negatively regulates fish IFN response by targeting MITA

Yu Zhou[a,d], Long-Feng Lu[a], Xiao-Bing Lu[a,d], Shun Li[a,*], Yong-An Zhang[a,b,c,**]

[a] Institute of Hydrobiology, Chinese Academy of Sciences, Wuhan, China
[b] State Key Laboratory of Agricultural Microbiology, College of Fisheries, Huazhong Agricultural University, Wuhan, China
[c] Laboratory for Marine Biology and Biotechnology, Qingdao National Laboratory for Marine Science and Technology, Qingdao, China
[d] University of Chinese Academy of Sciences, Beijing, China

ARTICLE INFO

Keywords:
cGAS-like
Negative regulator
Interferon
MITA
Grass carp

ABSTRACT

Mammalian cyclic GMP-AMP synthase (cGAS) senses double-stranded (ds) DNA in the cytosol to activate the innate antiviral response. In the present study, a cGAS-like gene, namely cGASL, was cloned from grass carp *Ctenopharyngodon idellus*, and its role as a negative regulator of the IFN response was revealed. Phylogenetic analysis indicated that cGASL was evolutionarily closest to cGAS, but was not a true ortholog of cGAS. Overexpression of cGASL inhibited poly I:C-stimulated grass carp (gc)IFN1pro and ISRE activities. In addition, MITA-, but not TBK1-mediated activation of gcIFN1pro was impaired by cGASL. Co-immunoprecipitation and Western blot experiments indicated that cGASL interacted with MITA and TBK1, resulting in a reduction in the phosphorylation of MITA. Lastly, overexpression of cGASL reduced the transcriptional levels of several IFN-stimulated genes activated by MITA. Collectively, these data suggest that cGASL is a negative regulator of IFN response by targeting MITA in fish.

1. Introduction

The innate immune system provides critical host defense against microbial infection [1,2]. Upon microbial infection, cellular pattern recognition receptors (PRRs) recognize the pathogen-associated molecular patterns (PAMPs), which are small molecular motifs conserved within groups of microbes, such as nucleic acids from viruses or bacteria, bacterial lipopolysaccharide (LPS), and peptidoglycan [1–3]. The PRRs then trigger a series of signaling events, leading to the induction of type I interferons (IFNs), pro-inflammatory cytokines, and other downstream effectors. In mammals, PRRs mainly comprise Toll-like receptors (TLRs), nucleotide-binding oligomerization domain (NOD)-like receptors (NLRs), retinoic acid-inducible gene I (RIG-I)-like receptors (RLRs), and a number of intracellular DNA sensors [1,2,4].

Viral nucleic acids are major PAMPs that are sensed by cellular PRRs after virus infection [4]. In the cytoplasm, the cyclic GMP-AMP synthase (cGAS) and RLRs including RIG-I and melanoma differentiation-associated gene 5 (MDA5) are the major PRRs responsible for sensing viral DNAs and RNAs, respectively [2,5–7]. After detecting the foreign nucleic acids, these receptors can transfer the signals to the downstream effector molecules mediator of IRF3 activation (MITA, also known as STING) and TANK-binding kinase 1 (TBK1) [8–11]. TBK1 then interacts with MITA, undergoes self-phosphorylation, and subsequently phosphorylates MITA, which is necessary for the recruitment of the IFN regulatory factor 3 (IRF3) [9,11–13]. In this complex, TBK1 further phosphorylates IRF3, which translocates to the nucleus to induce the expression of IFN. Tremendous progress in the understanding of fish IFN response provides evidence that the IFN antiviral response in fish is conserved with those in mammals [1,11,14–16]. For example, fish MITA plays a pivotal role in defending against both DNA and RNA

Abbreviations: cGAS, Cyclic GMP-AMP synthase; cGASL, cGAS-like; Co-IP, Coimmunoprecipitation; GCO, Grass carp ovary cell; IFI35, Interferon-induced protein 35; IFN, Interferon; IRF, IFN regulatory factor; ISG, IFN-stimulated gene; ISRE, IFN stimulated response element; LPS, Lipopolysaccharide; MAB21, Male Abnormal 21; MB21D1, MAB21 domain-containing protein 1; MAVS, Mitochondrial antiviral signaling protein; MDA5, Melanoma differentiation-associated gene 5; MITA, Mediator of IRF3 activation; Na_3VO_4, Sodium orthovanadate; NLR, Nucleotide-binding oligomerization domain (NOD)-like receptor; NMI, N-Myc and STAT interactor; NTase, Nucleotidyltransferase; ORF, Open reading frame; PBS, Phosphate-buffered saline; PAMP, pathogen-associated molecular pattern; PFA, Paraformaldehyde; PMSF, Phenylmethylsulfonyl fluoride; Poly I:C, Polyinosinic: Polycytidylic acid; PRR, Pattern recognition receptor; qPCR, Quantitative real-time PCR; RIG-I, Retinoic acid inducible gene I; RIPA, Radioimmunoprecipitation; RLR, RIG-I-like receptor; TBK1, TANK-binding kinase 1; TLR, Toll-like receptor; TM, Transmembrane motif

* Corresponding author.
** Corresponding author. Institute of Hydrobiology, Chinese Academy of Sciences, Wuhan, China.
E-mail addresses: bob@ihb.ac.cn (S. Li), yzhang@ihb.ac.cn (Y.-A. Zhang).

https://doi.org/10.1016/j.fsi.2019.10.010
Received 5 August 2019; Received in revised form 30 September 2019; Accepted 4 October 2019
Available online 06 October 2019
1050-4648/

viruses, and fish IRF3 needs to be phosphorylated by TBK1 to induce IFN expression [11,15,17].

The male abnormal 21 (MAB21) family belongs to the large and diverse superfamily of nucleotidyltransferase (NTase) fold proteins [18]. Five members of this family have been identified in humans, including MAB21-like protein 1 (MAB21L1), MAB21L2, MAB21L3, MAB21 domain-containing protein 1 (MB21D1, also known as cGAS), and MB21D2 [19]. The MAB21 proteins usually contain an NTase domain that partly overlaps with a C-terminal MAB21 domain. Functional studies revealed that most of the MAB21 family members are involved in cell fate determination and embryogenesis [20–22]. In *Caenorhabditis elegans*, the MAB21 protein is related to cell fate and the formation of sensory organs in male nematodes [20]. Several studies in model organisms *Danio rerio*, *Xenopus laevis,* and *Mus musculus* revealed that the vertebrate homologs of MAB21 protein such as MAB21L1 and MAB21L2 are important in embryonic tissue patterning and organogenesis [22–24]. Few studies have found evidence of the MAB21 members being involved in innate immune regulation. Mammalian cGAS was recently identified as a cytoplasmic DNA sensor in the immune system, capable of detecting cytosolic DNAs derived from various types of viruses [7]. After binding to double-stranded DNA (dsDNA), cGAS is activated and catalyzes the synthesis of cyclic GMP-AMP (cGAMP) from ATP and GTP [5,25]. Then, cGAMP serves as an endogenous second messenger to stimulate the production of IFN via MITA [7].

Although cGAS has been identified as a key component in the innate immune system, it is unclear whether other members of the MAB21 family can function in the IFN response. In this study, a cGAS-like gene, namely cGASL, was cloned from grass carp *Ctenopharyngodon idellus* and its role in the fish IFN response was determined. Phylogenetic analysis showed that cGASL was most similar to cGAS, but was not a true ortholog of cGAS. Functionally, cGASL could negatively regulate IFN and IFN-stimulated gene (ISG) production by interacting with MITA to reduce its phosphorylation mediated by TBK1. Our findings revealed a new negative regulatory mechanism for fish IFN response.

2. Materials and methods

2.1. Cell lines and transient transfection

Grass carp ovary (GCO) cells purchased from China Center For Type Culture Collection were maintained at 28 °C, 5% CO_2 in medium 199 (Invitrogen). HEK 293T cells were grown at 37 °C, 5% CO_2 in DMEM medium (Invitrogen). All mediums were supplemented with 10% fetal bovine serum (FBS, Invitrogen) and penicillin-streptomycin (100 U/ml). HEK 293T or GCO cells were seeded in 10 cm^2 dishes, 6 or 24-well plates and 24 h later were co-transfected with indicated plasmids by using X-tremeGENE HP DNA Transfection Reagent (Roche) according to the manufacturer's protocol.

2.2. Homologous cloning of the grass carp cGASL gene

Based on the predicted cGAS-like mRNA sequences in zebrafish *Danio rerio* (GenBank accession No.: XM_003200639.5), common carp *Cyprinus carpio* (XM_019125260.1) and crucian carp *Carassius auratus* (XM_026288623.1), degenerate primers were designed to amplify a partial fragment of cGASL from grass carp gut cDNA. The PCR protocol was as follows: 1 cycle of 95 °C/5 min; 35 cycles of 95 °C/30 s, 50 °C/30 s, 72 °C/2 min; 1 cycle of 72 °C/10 min. Amplified PCR products were ligated into pMD™18-T Vector, transformed into the competent *Escherichia coli* TOP10 cells, and plated on the LB-agar petri-dish. Positive colonies containing expected size insert were screened by colony PCR. Five of them were picked up and sent to a commercial company (Wuhan TSINGKE Biological Technology, China) for sequencing.

2.3. Full-length cGASL cDNA cloning and plasmid construction

Based on the obtained cDNA fragment of cGASL, 5′-RACE was performed using the reverse primers gccGASL-5R1 and gccGASL-5R2, while the 3′-RACE was performed using the forward primers gccGASL-3F1 and gccGASL-3F2 (Supplemental Table 1). The amplified PCR product was cloned and sequenced as described above. The full-length cDNA sequence was confirmed by sequencing the PCR product amplified by primers gccGASL-F and gccGASL-R (Supplemental Table 1) within the 5′ and 3′ untranslated regions respectively. The open reading frame (ORF) of grass carp cGASL, MAVS (mitochondrial antiviral signaling protein, KF366908.1), MITA (NM_001278837.1) and TBK1 (NM_001044748.2) were subcloned into pcDNA3.1 (+) (Invitrogen), pCMV-HA and pCMV-Myc (BD Clontech), respectively. For subcellular localization, the ORF of grass carp cGASL was inserted into pEGFP-N3 vector (BD Clontech), and the ORF of grass carp MITA and TBK1 were subcloned into pCS2-mCherry vector (BD Clontech). The grass carp (gc) IFN1 promoter was obtained from NCBI database (GU139255.1) and cloned into pGL3-Basic luciferase reporter vector (Promega). The plasmid containing ISRE-Luc in pGL3-Basic luciferase reporter vector was constructed as previously described [26]. The *Renilla* luciferase internal control vector (pRL-TK) was purchased from Promega. All constructs were confirmed by DNA sequencing. The primers including the restriction enzyme cutting sites used for plasmid construction are listed in Supplemental Table 1.

2.4. Sequence alignment and phylogenetic analysis

The molecular mass and protein domains of the deduced amino acid sequences were analyzed by Expert Protein Analysis System (ExPasy) (http://www.expasy.org/) and Simple Modular Architecture Research Tool (SMART) (http://smart.embl-heidelberg.de/), respectively. For phylogenetic analysis, sequences of MAB21 proteins were obtained from GenBank. The amino acid sequences were aligned using the GeneDoc software, and the phylogenetic tree was constructed based on the maximum likelihood (ML) approach which was bootstrapped 1000 times using the MEGA 6.0 software.

2.5. Luciferase activity assay

GCO cells were seeded into 24-well plates and 24 h later were co-transfected with 0.25 μg luciferase reporter plasmid (gcIFN1pro-Luc or ISRE-Luc) and 0.05 μg of *Renilla* luciferase internal control vector (pRL-TK). The pRL-TK was used to normalize the transcriptional levels induced by the promoters and the empty vector pcDNA3.1 (+) was used to maintain equivalent amounts of DNA in each well. Stimulation with poly I:C was done 24 h later. At 48 h post-transfection, the cells were washed with phosphate-buffered saline (PBS) and lysed for measuring luciferase activity using the Dual-Luciferase Reporter Assay System according to the manufacturer's instructions (Promega). The results for each experiment were representative of more than three independent experiments, each performed in triplicate.

2.6. RNA extraction, reverse transcription, and quantitative real-time PCR

The total RNAs of GCO cells and tissues from three apparently healthy grass carps were extracted using the Trizol reagent (Invitrogen). The ten tissues included brain, eye, gill, heart, liver, spleen, gut, trunk kidney, muscle, and skin. First-strand cDNA was synthesized using a GoScript Reverse Transcription System (Promega) according to the manufacturer's instructions. Quantitative real-time PCR (qPCR) was performed with Fast SYBR Green master mix (Bio-Rad) on the CFX96 Real-Time System (Bio-Rad). PCR conditions were as follows: 95 °C for 5 min, then 45 cycles of 95 °C for 20 s, 60 °C for 20 s, 72 °C for 30 s and the β-actin primers were used to normalize the data. All primers used for qPCR are shown in Supplemental Table 1. The

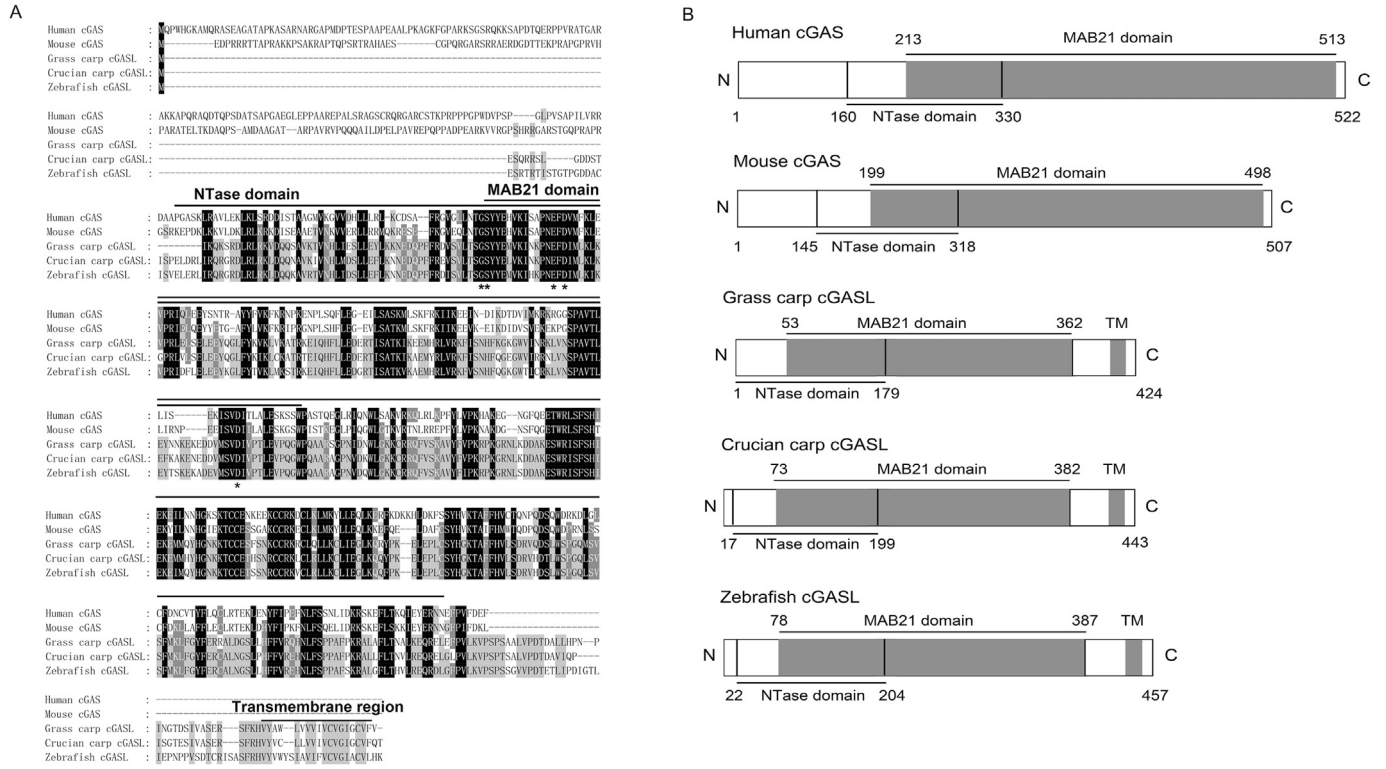

Fig. 1. Characterization of mammalian cGAS and fish cGASL proteins. (A) Multiple alignment of the amino acid sequences of cGAS and cGASL proteins using GeneDoc. The NTase domain, MAB21 domain, and transmembrane region were indicated by lines, and five asterisks indicated key catalytic residues within the NTase domain. (B) Schematic representation of mammalian cGAS and fish cGASL proteins.

specificity of the PCR amplification for all primer sets was verified from the dissociation curves. The identity of each PCR products was confirmed by sequencing at Wuhan TSINGKE Biological Technology Inc. The relative fold changes were calculated using the $2^{-\Delta\Delta Ct}$ method. Three independent experiments were conducted for statistical analysis.

2.7. Coimmunoprecipitation assay

For the coimmunoprecipitation (Co-IP) experiments, HEK 293T cells seeded into 10 cm^2 dishes overnight were transfected with a total of 10 μg of the indicated plasmids. At 24 h post-transfection, the medium was removed and the cell monolayer was washed twice with 10 ml ice-cold PBS. The cells were then lysed in 1 ml radioimmunoprecipitation (RIPA) lysis buffer (1% NP-40, 50 mM Tris-HCl, pH 7.5, 150 mM NaCl, 1 mM EDTA, 1 mM NaF, 1 mM sodium orthovanadate [Na_3VO_4], 1 mM phenylmethylsulfonyl fluoride [PMSF], 0.25% sodium deoxycholate) containing a protease inhibitor cocktail (Sigma-Aldrich) at 4 °C for 1 h on a rocker platform. The cellular debris was removed by centrifugation at 12,000 × *g* for 15 min at 4 °C. The supernatant was transferred to a fresh tube and incubated with 20 μl anti-hemagglutinin (HA)-agarose beads (Sigma-Aldrich) overnight at 4 °C with constant agitation. These samples were further analyzed by immunoblotting. Immunoprecipitated proteins were collected by centrifugation at 5000 X *g* for 1 min at 4 °C, washed three times with lysis buffer, and re-suspended in 50 μl 2 × SDS sample buffer. The immunoprecipitates and whole-cell lysates were analyzed by immunoblotting with the indicated antibodies (Abs).

2.8. Immunoblot analysis

Immunoprecipitates or whole-cell extracts were separated by 9% SDS-PAGE and transferred to polyvinylidene difluoride (PVDF) membrane (Bio-Rad). The membranes were blocked for 1 h at room temperature in TBST buffer (25 mM Tris-HCl, 150 mM NaCl, 0.1% Tween 20, pH 7.5) containing 5% nonfat dry milk, probed with the indicated primary Abs at an appropriate dilution overnight at 4 °C, washed three times with TBST, and then incubated with secondary Abs for 1 h at room temperature. After three additional washes with TBST, the membranes were stained with the Immobilon Western chemiluminescent horseradish peroxidase (HRP) substrate (Millipore) and detected using an ImageQuant LAS 4000 system (GE Healthcare). Abs were diluted as follows: anti-β-actin (Cell Signaling Technology) and anti-Flag/HA/Myc (Sigma-Aldrich) at 1:3,000, and HRP-conjugated anti-mouse IgG (Thermo Scientific) at 1:5000. Results are representative of data from three independent experiments.

2.9. Fluorescent microscopy

GCO cells were plated onto coverslips in 6-well plates and transfected with indicated plasmids for 24 h. Then the cells were washed twice with PBS and fixed with 4% paraformaldehyde (PFA) for 1 h. After draining the fixative, the cells were stained with DAPI (1 mg/ml; Beyotime) for 30 min in dark at room temperature. Finally, the coverslips were washed and observed with a confocal microscope under a 63 × oil immersion objective (SP8; Leica Microsystems).

2.10. Statistics analysis

The results are expressed as mean ± SDs of at least three independent experiments ($n \geq 3$). Data were analyzed using a Student's unpaired t-tests. A p value < 0.05 was considered to be statistically significant.

3. Results

3.1. Sequence characterization of grass carp cGASL

The obtained full length cDNA of grass carp cGASL was 1682-bp

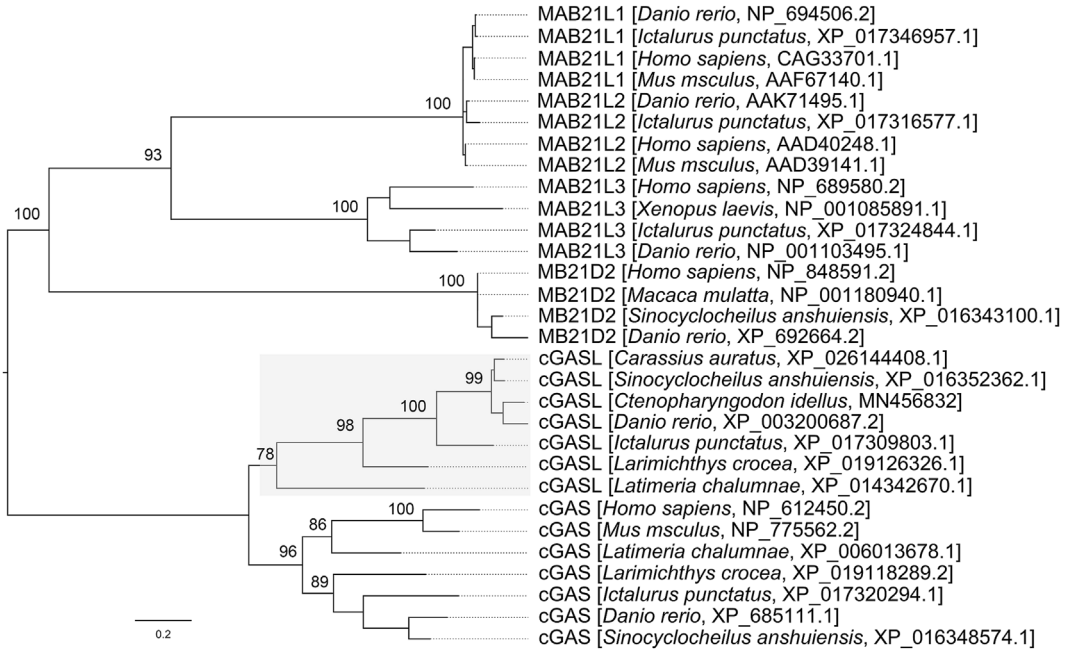

Fig. 2. Phylogenetic analysis of grass carp cGASL and the other MAB21 proteins. The tree was constructed by ML method supported with 1000 bootstrap replications using MEGA 6.0 software. The numbers at a node reflect the bootstrap values.

long (MN456832) and included a predicted ORF of 1275 bp, a 206-bp 5′-untranslated region (UTR), and a 201-bp 3′-UTR. The ORF encoded a putative 424-aa protein with a calculated molecular mass of 46.64 kDa and a pI of 9.96. Multiple amino acid sequence alignments revealed that grass carp cGASL contained an NTase domain, a MAB21 domain, and a C-terminal transmembrane (TM) region (Fig. 1A and B). Five conserved key catalytic residues (G52, S53, E65, D67, and D168) were observed in the NTase domain (Fig. 1A). Phylogenetic analysis showed that grass carp cGASL grouped together with the other fish cGASLs, and they were most similar to fish and mammalian cGAS proteins, which clustered in a well-supported group (Fig. 2).

3.2. Tissue expression pattern of grass carp cGASL in healthy fish

To characterize the tissue expression pattern of grass carp cGASL at the mRNA level, the total RNA for ten tissue samples from healthy grass carp was extracted and examined by qRT-PCR. As shown in Fig. 3, grass carp cGASL expression was significantly high in the liver and gut tissues; moderately high in the muscle, trunk kidney, skin, and gill tissues; and poor in the heart, spleen, brain, and eye tissues.

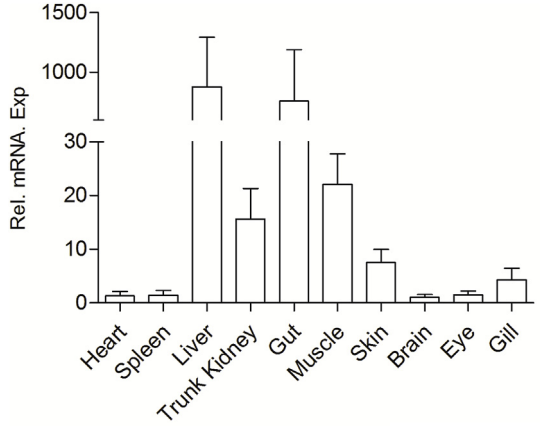

Fig. 3. Tissue distribution of cGASL. Transcriptional levels of cGASL were detected by qPCR and normalized to ß-actin. Graphs show mean ± SD, and the experiments were repeated for three times with similar results.

3.3. cGASL inhibits MITA-mediated gcIFN1pro activities

Due to the close relationship between grass carp cGASL and mammalian cGAS proteins, we hypothesized that cGASL may play a role in the IFN response. Therefore, luciferase assays were performed to investigate the potential of cGASL to affect gcIFN1pro and ISRE activities. As shown in Fig. 4A and B, poly I:C infection induced substantial activation of gcIFN1pro and ISRE, but the transfection of cGASL alone had no effect on the activation of gcIFN1pro and ISRE relative to the transfection of the empty pcDNA3.1 vector. However, the gcIFN1pro and ISRE activities stimulated by poly I:C were significantly impeded by cGASL overexpression in a dose-dependent manner, which suggested that cGASL inhibits the activation of IFNϕ1pro and ISRE upon infection with poly I:C.

Since RLR signaling is involved in the poly I:C-triggered IFN response [11,14], the relationship between cGASL and RLR molecules was examined with luciferase assays. As shown in Fig. 4C, overexpression of RLR molecules upregulated gcIFN1pro activity, but the capabilities of MAVS and MITA to activate gcIFN1pro decreased significantly during the overexpression of cGASL, while that of TBK1 was unaffected. The inhibitory effect of cGASL on MITA-stimulated gcIFN1pro and ISRE activities was further verified through dose-dependent experiments (Fig. 4D and E). Given that MITA is downstream of MAVS, these results suggested that cGASL likely decreased the gcIFN1pro activity via the negative regulation of MITA.

3.4. cGASL interacts with MITA to decrease its phosphorylation induced by TBK1

In mammals and fish, MITA is a mediator protein which migrates in cells and recruits TBK1, promoting the phosphorylation of IRF3. In this process, MITA associates with and is phosphorylated by TBK1, which is crucial for the recruitment of IRF3 [11,13]. Given that MITA-induced gcIFN1pro and ISRE activities were attenuated by cGASL, it was necessary to investigate whether cGASL associates with MITA and TBK1. As shown in Fig. 5A, B, and C, grass carp TBK1 associated with MITA, and interactions between cGASL and MITA or TBK1 were also

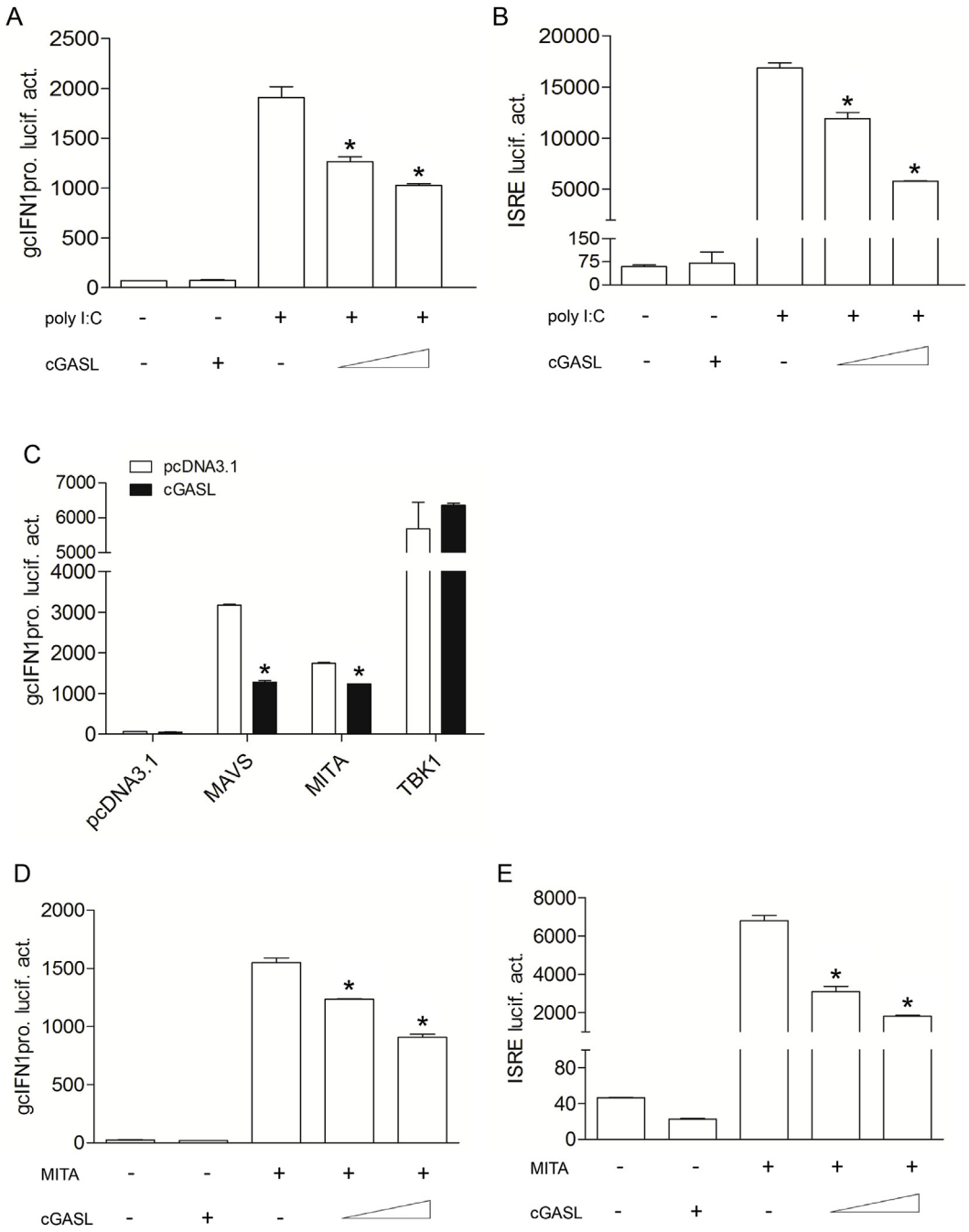

Fig. 4. Inhibition of gcIFN1pro activity by overexpression of cGASL. (A and B) Overexpression of cGASL inhibited the poly I:C-triggered gcIFN1pro and ISRE activities in a dose-dependent manner. GCO cells were seeded in 24-well plates overnight and co-transfected with 250 ng gcIFN1pro-Luc (A) or ISRE-Luc (B) and 25 ng pRL-TK, plus pcDNA3.1-cGASL (0, 250, 0, 200 or 400 ng/well). At 24 h post-transfection, cells were treated with poly I:C (1 μg/ml). After 24 h stimulation, the cell lysates were harvested for luciferase assay. (C) cGASL blocked RLR-mediated activation of the gcIFN1 promoter. GCO cells were seeded in 24-well plates overnight and co-transfected with pcDNA3.1-MAVS, pcDNA3.1-MITA or pcDNA3.1-TBK1 and pcDNA3.1-cGASL plus gcIFN1pro-Luc at a ratio of 1:1:1. At 24 h post-transfection, cells were collected for detection of luciferase activities. (D and E) Overexpression of cGASL inhibited MITA-induced gcIFN1pro and ISRE activities in a dose-dependent manner. GCO cells were seeded in 24-well plates overnight and co-transfected with 250 ng gcIFN1pro-Luc (D) or ISRE-Luc (E), 25 ng pRL-TK, 250 ng pcDNA3.1-MITA, plus pcDNA3.1-cGASL (0, 250, 0, 200 or 400 ng/well). The luciferase activities were monitored at 24 h after transfection. Error bars are the SDs obtained by measuring each sample in triplicate. Asterisks indicate significant differences from control (*$p < 0.05$).

confirmed. These results suggested that cGASL, MITA, and TBK1 form a protein complex in the RLR pathway.

We further investigated whether cGASL affects TBK1-induced phosphorylation of MITA. Fig. 5D shows that when HA-MITA was co-transfected with HA-TBK1, a shifted band with higher molecular weight could be detected by the anti-HA Ab, which was the phosphorylated MITA; however, when Flag-cGASL was co-transfected with HA-MITA and HA-TBK1, the TBK1-mediated phosphorylation of MITA decreased. These results demonstrated that cGASL reduced the phosphorylation of MITA induced by TBK1.

3.5. cGASL decreases MITA-upregulated IFN-stimulated genes

Given that cGASL interacted with MITA to reduce its phosphorylation induced by TBK1, the effect of cGASL on MITA-stimulated expression of ISGs was investigated at the mRNA level. GCO cells were co-

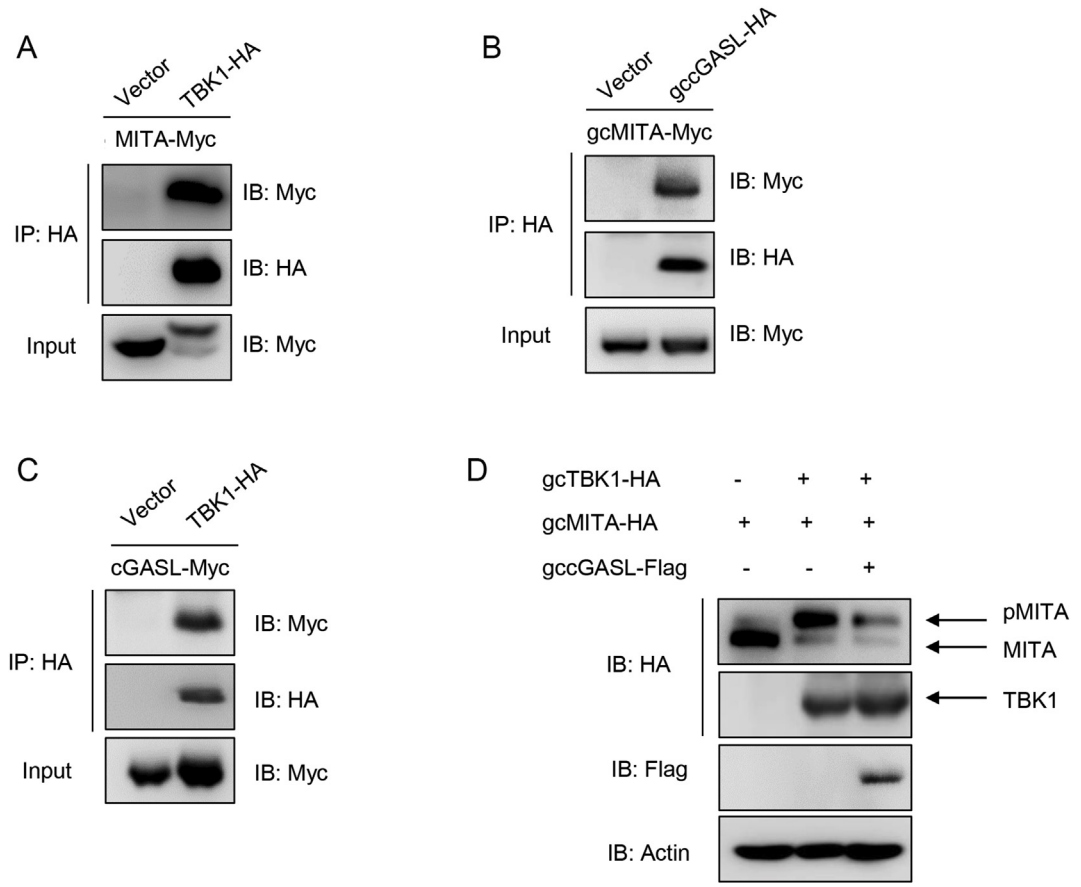

Fig. 5. Effects of cGASL on the phosphorylation of MITA mediated by TBK1. (A) TBK1 interacted with MITA. 293T cells seeded in 10 cm^2 dishes were transfected with the plasmids indicated (5 μg each). After 24 h, cell lysates were immunoprecipitated (IP) with anti-HA-agarose beads. The immunoprecipitates and cell lysates were then analyzed by immunoblotting (IB) with the anti-Myc Abs. (B and C) cGASL interacted with MITA and TBK1. 293T cells seeded in 10 cm^2 dishes were transfected with the plasmids indicated (5 μg each). After 24 h, IP and IB analyses were performed with the Abs indicated. (D) cGASL decreased TBK1-mediated phosphorylation of MITA. 293T cells were seeded in 6-well plates overnight and transfected with the plasmids indicated (1 μg each) for 24 h. Whole-cell lysates were subjected to IB with the anti-HA, anti-Flag and anti-ß-actin Abs.

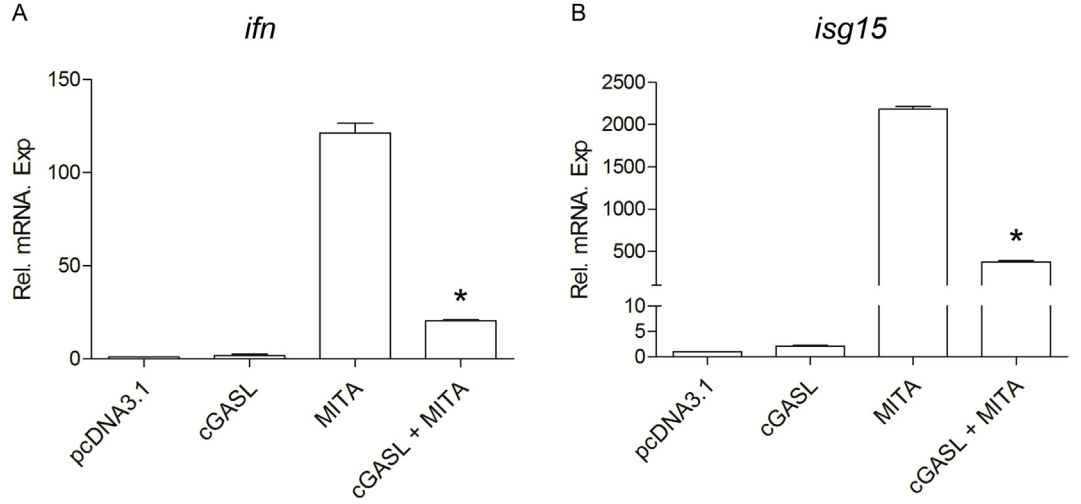

Fig. 6. Effect of cGASL on the expression of ISGs. GCO cells were seeded in 6-well plates overnight and co-transfected with 1 μg pcDNA3.1-cGASL or pcDNA3.1 (control vector) and 1 μg pcDNA3.1-MITA. At 24 h post-transfection, the total RNAs were extracted to examine the transcripts of *ifn* (A) and *isg15* (B) of GCO cells by qPCR. ß-actin was used as an internal control for normalization. Error bars are the SDs obtained by conducting three individual experiments. Asterisks indicate significant differences from control (*$p < 0.05$).

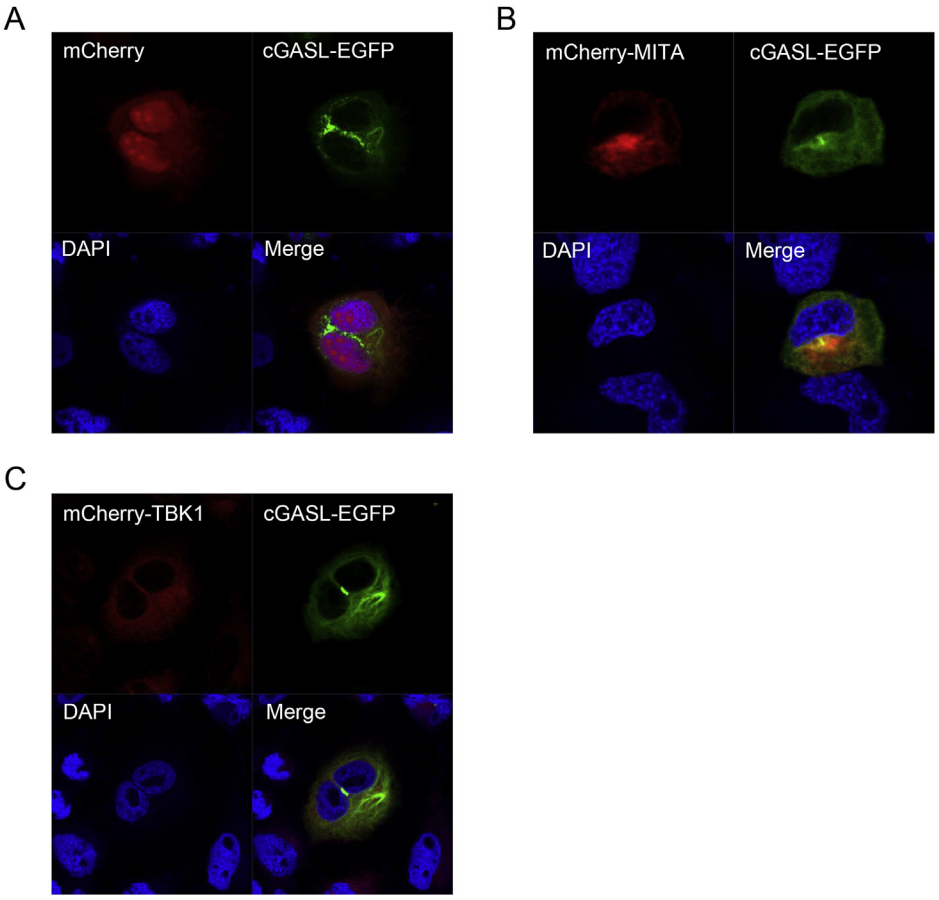

Fig. 7. Subcellular localization of cGASL. GCO cells seeded on microscopy coverglass in six-well plates were transfected with 1 μg of cGASL-EGFP and 1 μg of empty vector (A), mCherry-MITA (B) or mCherry-TBK1 (D). After 24 h, the cells were fixed and subjected to confocal microscopy analysis. Green signals represent overexpressed cGASL protein, red signals represent overexpressed MITA or TBK1, and blue staining indicates the nucleus region. The yellow staining in the merged images indicates colocalization of cGASL and MITA or TBK1 (original magnification, 63 × oil immersion objective). All experiments were repeated at least three times with similar results. (For interpretation of the references to colour in this figure legend, the reader is referred to the Web version of this article.)

transfected with pcDNA3.1-MITA and pcDNA3.1-cGASL or an empty vector, and the total RNAs were extracted and evaluated with qPCR. As shown in Fig. 6, cGASL transfection did not induce the expression of *ifn* and *isg15*, consistent with the results in the control group. When MITA was overexpressed, the transcription of these ISGs was remarkably upregulated, while the induction was significantly decreased by co-transfection with cGASL (Fig. 6).

3.6. Subcellular localization of grass carp cGASL

To further investigate the function of cGASL, its subcellular location was investigated in GCO cells. Confocal microscopy revealed that the cGASL-EGFP signal was mainly distributed in the cytoplasm (Fig. 7A). We co-transfected mCherry-MITA or mCherry-TBK1 with cGASL-EGFP. Red fluorescence from MITA and TBK1 was observed in the cytosol, but cGASL (green) was not colocalized with MITA and TBK1 (Fig. 7B and C).

4. Discussion

Although IFNs and ISGs are critical components in the host defense against viral infection, uncontrolled induction of IFNs and ISGs can lead to a number of diseases. Therefore, multiple negative regulatory mechanisms are utilized by the host to avoid excessive activation of the IFN response. Here, we report a new mechanism for the negative regulation of IFN and ISG production by a cGAS-like gene in fish.

Previous studies on MAB21 proteins have mainly focused on their roles in animal development [20–24] and few studies have found evidence of their involvement in the innate immune response. Mammalian cGAS was recently identified as a ubiquitous sensor for cytosolic dsDNA, which plays a critical role in innate immune responses to cytosolic DNA and various DNA viruses [5,7,25]. Consequently, the question of whether fish cGAS or other MAB21 proteins can function in innate immune regulation has attracted great interest. Grass carp cGASL was obtained based on the predicted fish cGAS-like sequences. Despite the close evolutionary relationship between the cGASL and cGAS proteins, fish cGASLs formed a single clade in the phylogenetic tree while mammalian and fish cGASs clustered in another group. Furthermore, structural differences were identified between cGASL and cGAS. Although both cGAS and cGASL proteins contained an NTase and an MAB21 domain, the NTase domain in cGASL was located on the N-terminus while the corresponding domain in cGAS was not. Moreover, a predicted transmembrane region was located at the C-terminus of cGASL, which was absent in cGAS. These data indicated that the fish cGASL proteins are not orthologs of the mammalian cGAS proteins.

Due to the close relationship between cGAS and cGASL, we speculated that cGASL is related to the regulation of the IFN response. In the luciferase assays we performed, poly I:C-stimulated gcIFN1pro and ISRE activities were reduced by cGASL, suggesting that cGASL is able to negatively regulate IFN expression.

The RLR signaling pathway plays a major role in driving type I IFN production and antiviral gene expression to initiate and modulate antiviral immunity. Aberrant RLR signaling or the dysregulation of RLR expression is known to be related to the development of various autoimmune syndromes [27]. In mammals, a series of negative molecules have been reported to regulate the RLR pathway in order to avoid excessive IFN production. IFN-induced protein 35 (IFI35) interacts with RIG-I and negatively regulates its activation through mechanisms including the suppression of dephosphorylation activation of RIG-I and proteasome-mediated degradation of RIG-I [28]. ISG56 (IFIT1) was found to associate with MITA and inhibit its interactions with MAVS and TBK1 to negatively regulate the IFN response [29]. IFN-induced N-Myc and STAT interactor (NMI) associates with IRF7, leading to K48-linked ubiquitination and proteasomal degradation of IRF7 [30]. In

recent years, negative regulators of the RLR system have also been identified in fishes. For example, fish A20 (also known as tumor necrosis factor alpha-induced protein 3 or TNFAIP3) interrupts RIG-I signaling by targeting TBK1 [31]; FTRCA1 (a crucian carp-specific finTRIM gene) associates with TBK1 and results in autophage-lysosomal degradation of TBK1 [32]; and zebrafish IRF10 inhibits IFN production by binding to the promoter of IFN and interacting with MITA [33]. In the current study, grass carp cGASL was likely to target MITA to inhibit the IFN response. Indeed, MITA is a critical mediator protein in the innate immune system. It was reported that TBK1-mediated phosphorylation of MITA was required for IRF3 activation, and knockdown of MITA severely inhibited virus-triggered IRF3 activation and type I IFN expression [13]. The interaction between cGASL and the MITA-TBK1 complex may partly hinder the phosphorylation process mediated by TBK1, resulting in the reduction of MITA phosphorylation.

The negative regulation function of cGASL in the innate immune system might be further reflected by its expression profile. In this investigation, grass carp cGASL had the highest expression in the liver and gut, which was significantly higher than that in other tissues. It is noteworthy that a previous study conducted in zebrafish also identified the liver and gut as the main sites for ISG expression during viral infection [34]. Therefore, we speculated that the high expression of cGASL at these sites might be a strategy for a balanced antiviral immune response to avoid excessive induction of ISGs.

The cGASL proteins were most similar to cGAS proteins. Although cGAS has been demonstrated to be a critical component in the STING (or MITA) signaling pathway in mammals, its role is less clear in fishes. It was reported that zebrafish cGAS was dispensable in the STING-mediated immune response against Herpes simplex virus 1 (HSV-1) [35]. However, a recent study performed in Japanese medaka *Oryzias latipes* showed that fish cGAS may be more important for the immune response to bacterial DNA than other DNA sensors [36]. Further studies are needed to determine the role of fish cGAS in the antiviral innate immune response. As for the other MAB21 proteins, it is also recommended to determine whether they are involved in the innate immune response.

In summary, this study demonstrated that grass carp cGASL is a negative regulator of the RLR pathway. It interacts with MITA, and reduces the phosphorylation of MITA induced by TBK1 to negatively regulate the MITA-mediated IFN response.

Declaration of competing interest

The authors have no conflicting commercial or financial interest in publishing this paper.

Acknowledgments

This work was supported by the National Natural Science Foundation of China (31725026, 31502200) and the Science Fund for Creative Research Groups of the Natural Science Foundation of Hubei Province of China (2018CFA011).

Appendix A. Supplementary data

Supplementary data to this article can be found online at https://doi.org/10.1016/j.fsi.2019.10.010.

References

[1] S.N. Chen, P.F. Zou, P. Nie, Retinoic acid-inducible gene I (RIG-I)-like receptors (RLRs) in fish: current knowledge and future perspectives, Immunology 151 (1) (2017) 16–25.
[2] M. Yoneyama, K. Onomoto, M. Jogi, T. Akaboshi, T. Fujita, Viral RNA detection by RIG-I-like receptors, Curr. Opin. Immunol. 32 (2015) 48–53.
[3] M.J. McFadden, N.S. Gokhale, S.M. Horner, Protect this house: cytosolic sensing of viruses, Curr. Opin.Virol. 22 (2017) 36–43.
[4] H.H. Hoffmann, W.M. Schneider, C.M. Rice, Interferons and viruses: an evolutionary arms race of molecular interactions, Trends Immunol. 36 (3) (2015) 124–138.
[5] X. Li, C. Shu, G. Yi, C.T. Chaton, C.L. Shelton, J. Diao, X. Zuo, C.C. Kao, A.B. Herr, P. Li, Cyclic GMP-AMP synthase is activated by double-stranded DNA-induced oligomerization, Immunity 39 (6) (2013) 1019–1031.
[6] J.J. Wu, W. Li, Y. Shao, D. Avey, B. Fu, J. Gillen, T. Hand, S. Ma, X. Liu, W. Miley, A. Konrad, F. Neipel, M. Sturzl, D. Whitby, H. Li, F. Zhu, Inhibition of cGAS DNA sensing by a herpesvirus virion protein, Cell Host Microbe 18 (3) (2015) 333–344.
[7] L. Sun, J. Wu, F. Du, X. Chen, Z.J. Chen, Cyclic GMP-AMP synthase is a cytosolic DNA sensor that activates the type I interferon pathway, Science 339 (6121) (2013) 786.
[8] E. Lam, S. Stein, E. Falck-Pedersen, Adenovirus detection by the cGAS/STING/TBK1 DNA sensing cascade, J. Virol. 88 (2) (2014) 974–981.
[9] Q. Chen, L. Sun, Z.J. Chen, Regulation and function of the cGAS-STING pathway of cytosolic DNA sensing, Nat. Immunol. 17 (10) (2016) 1142–1149.
[10] A. Zevini, D. Olagnier, J. Hiscott, Crosstalk between cytoplasmic RIG-I and STING sensing pathways, Trends Immunol. 38 (3) (2017) 194–205.
[11] F. Sun, Y.B. Zhang, T.K. Liu, J. Shi, B. Wang, J.F. Gui, Fish MITA serves as a mediator for distinct fish IFN gene activation dependent on IRF3 or IRF7, J. Immunol. 187 (5) (2011) 2531–2539.
[12] M.M. Hu, Q. Yang, X.Q. Xie, C.Y. Liao, H. Lin, T.T. Liu, L. Yin, H.B. Shu, Sumoylation promotes the stability of the DNA sensor cGAS and the adaptor STING to regulate the kinetics of response to DNA Virus, Immunity 45 (3) (2016) 555–569.
[13] B. Zhong, Y. Yang, S. Li, Y.Y. Wang, Y. Li, F. Diao, C. Lei, X. He, L. Zhang, P. Tien, H.B. Shu, The adaptor protein MITA links virus-sensing receptors to IRF3 transcription factor activation, Immunity 29 (4) (2008) 538–550.
[14] Y.B. Zhang, J.F. Gui, Molecular regulation of interferon antiviral response in fish, Dev. Comp. Immunol. 38 (2) (2012) 193–202.
[15] F. Sun, Y.B. Zhang, T.K. Liu, L. Gan, F.F. Yu, Y. Liu, J.F. Gui, Characterization of fish IRF3 as an IFN-inducible protein reveals evolving regulation of IFN response in vertebrates, J. Immunol. 185 (12) (2010) 7573–7582.
[16] F.F. Yu, Y.B. Zhang, T.K. Liu, Y. Liu, F. Sun, J. Jiang, J.F. Gui, Fish virus-induced interferon exerts antiviral function through Stat 1 pathway, Mol. Immunol. 47 (14) (2010) 2330–2341.
[17] R. Ge, Y. Zhou, R. Peng, R. Wang, M. Li, Y. Zhang, C. Zheng, C. Wang, Conservation of the STING-mediated cytosolic DNA sensing pathway in zebrafish, J. Virol. 89 (15) (2015) 7696–7706.
[18] K. Kuchta, L. Knizewski, L.S. Wyrwicz, L. Rychlewski, K. Ginalski, Comprehensive classification of nucleotidyltransferase fold proteins: identification of novel families and their representatives in human, Nucleic Acids Res. 37 (22) (2009) 7701–7714.
[19] C.C. de Oliveira Mann, R. Kiefersauer, G. Witte, K.P. Hopfner, Structural and biochemical characterization of the cell fate determining nucleotidyltransferase fold protein MAB21L1, Sci. Rep. 6 (2016) 27498.
[20] S.H. Ho, G.M. So, K.L. Chow, Postembryonic expression of *Caenorhabditis elegans* mab-21 and its requirement in sensory ray differentiation, Dev. Dynam. 221 (4) (2001) 422–430.
[21] R. Yamada, Y. Mizutani-Koseki, H. Koseki, N. Takahashi, Requirement for Mab21l2 during development of murine retina and ventral body wall, Dev. Biol. 274 (2) (2004) 295–307.
[22] R.L. Wong, K.L. Chow, Depletion of Mab21l1 and Mab21l2 messages in mouse embryo arrests axial turning, and impairs notochord and neural tube differentiation, Teratology 65 (2) (2002) 70–77.
[23] T. Kudoh, I.B. Dawid, Zebrafish mab21l2 is specifically expressed in the presumptive eye and tectum from early somitogenesis onwards, Mech. Dev. 109 (1) (2001) 95–98.
[24] G.T.C. Lau, O.G.W. Wong, P.M.Y. Chan, K.-H. Kok, R.L.Y. Wong, K.-T. Chin, M.C.M. Lin, H.-F. Kung, K.L. Chow, Embryonic XMab21l2 expression is required for gastrulation and subsequent neural development, Biochem. Biophys. Res. Commun. 280 (5) (2001) 1378–1384.
[25] E.J. Diner, D.L. Burdette, S.C. Wilson, K.M. Monroe, C.A. Kellenberger, M. Hyodo, Y. Hayakawa, M.C. Hammond, R.E. Vance, The innate immune DNA sensor cGAS produces a noncanonical cyclic dinucleotide that activates human STING, Cell Rep. 3 (5) (2013) 1355–1361.
[26] L.F. Lu, S. Li, X.B. Lu, S.E. LaPatra, N. Zhang, X.J. Zhang, D.D. Chen, P. Nie, Y.A. Zhang, Spring viremia of carp virus N protein suppresses fish IFNϕ1 production by targeting the mitochondrial antiviral signaling protein, J. Immunol. 196 (9) (2016) 3744–3753.
[27] Y.M. Loo, M. Gale Jr., Immune signaling by RIG-I-like receptors, Immunity 34 (5) (2011) 680–692.
[28] A. Das, P.X. Dinh, D. Panda, A.K. Pattnaik, Interferon-inducible protein IFI35 negatively regulates RIG-I antiviral signaling and supports vesicular stomatitis virus replication, J. Virol. 88 (6) (2014) 3103–3113.
[29] Y. Li, C. Li, P. Xue, B. Zhong, A.-P. Mao, Y. Ran, H. Chen, Y.-Y. Wang, F. Yang, H.-B. Shu, ISG56 is a negative-feedback regulator of virus-triggered signaling and cellular antiviral response, Proc. Natl. Acad. Sci. 106 (19) (2009) 7945.
[30] J. Wang, B. Yang, Y. Hu, Y. Zheng, H. Zhou, Y. Wang, Y. Ma, K. Mao, L. Yang, G. Lin, Y. Ji, X. Wu, B. Sun, Negative regulation of Nmi on virus-triggered type I IFN production by targeting IRF7, J. Immunol. 191 (6) (2013) 3393–3399.
[31] E. Merour, R. Jami, A. Lamoureux, J. Bernard, M. Bremont, S. Biacchesi, A20 (tnfaip3) is a negative feedback regulator of RIG-I-mediated IFN induction in teleost, Fish Shellfish Immunol. 84 (2019) 857–864.
[32] M. Wu, X. Zhao, X.Y. Gong, Y. Wang, J.F. Gui, Y.B. Zhang, FTRCA1, a species-specific member of finTRIM family, negatively regulates fish IFN response through autophage-lysosomal degradation of TBK1, J. Immunol. 202 (8) (2019) 2407–2420.
[33] S. Li, L.F. Lu, H. Feng, N. Wu, D.D. Chen, Y.B. Zhang, J.F. Gui, P. Nie, Y.A. Zhang,

IFN regulatory factor 10 is a negative regulator of the IFN responses in fish, J. Immunol. 193 (3) (2014) 1100–1109.
[34] V. Briolat, L. Jouneau, R. Carvalho, N. Palha, C. Langevin, P. Herbomel, O. Schwartz, H.P. Spaink, J.P. Levraud, P. Boudinot, Contrasted innate responses to two viruses in zebrafish: insights into the ancestral repertoire of vertebrate IFN-stimulated genes, J. Immunol. 192 (9) (2014) 4328–4341.
[35] R. Ge, Y. Zhou, R. Peng, R. Wang, M. Li, Y. Zhang, C. Zheng, C. Wang, Conservation of the STING-mediated cytosolic DNA sensing pathway in zebrafish, J. Virol. 89 (15) (2015) 7696–7706.
[36] S. Murakami, N. Morimoto, T. Kono, M. Sakai, J.I. Hikima, Molecular characterization and expression of the teleost cytosolic DNA sensor genes cGAS, LSm14A, DHX9, and DHX36 in Japanese medaka, *Oryzias latipes*, Dev. Comp. Immunol. 99 (2019) 103402.